Swirling Flows in Typical Combustor Geometries

David G. Lilley*
Oklahoma State University, Stillwater, Oklahoma

The aerodynamic aspects of swirling airflow expanding into a round-sectioned test section have recently been the subject of intensive research at Oklahoma State University. Studies were concerned with experimental and theoretical research on two-dimensional axisymmetric geometries under low-speed nonreacting, turbulent, swirling flow conditions typical of gas turbine and ramjet combustion chambers. They included recirculation zone characterization, time-mean and turbulence simulation in swirling recirculating flow, sudden and gradual expansion flowfields, and further complexities and parameter influences. The study included the investigation of a complete range of swirl strengths, swirler performance, downstream contraction nozzle sizes and locations, expansion ratios, and inlet side-wall angles. Their individual and combined effects on the test section flowfield were observed, measured, characterized, and predicted. Experimental methods included flow visualization (with smoke and neutrally buoyant helium-filled soap bubbles), five-hole pitot probe time-mean velocity field measurements, and single-, double- and triple-wire hot-wire anemometry measurements of time-mean velocities, normal and shear Reynolds streses. Computational methods included development of the STARPIC code from the primitive TEACH computer code, and STARPIC's use in flowfield prediction and turbulence model development. The present paper reviews the activity and highlights key results obtained during the study.

I. Introduction

The Problem

BOTH experimental and theoretical studies assist in the design and development of gas-turbine combustion chambers. Up to now, designers have relied heavily on experimental evidence to produce empirical formulas. However, traditional design methods are now being supplemented by analytical methods (numerical solution of the appropriate governing partial differential equations). Computer modeling of combustion processes is now an established fact, but improvements and new developments—both experimental and theoretical—can and should be made, with theoretical modeling being aided by carefully chosen experiments.

The accuracy of currently available prediction codes for swirling recirculating confined flows is in doubt because of questionable turbulence models and lack of a suitable experimental data base. A prerequisite to the prediction of more complex turbulent reacting flows is the development of suitable turbulence models and computer programs for flow prediction under nonreacting conditions, with which the present study is concerned.

Objectives

The recently completed research encompassed steady turbulent flow in two-dimensional axisymmetric geometries under low speed and nonreacting conditions. The particular problem addressed was concerned with turbulent flow in a round pipe entering an expansion into another round pipe. The inlet flow may possess a swirl component of velocity via passage through swirl vanes at an angle ϕ, and the side wall may slope at an angle α to the main flow direction. The resulting main flowfield domain may possess a central toroidal recirculation zone (CRTZ) in the middle of the region on the axis, in addition to the possibility of a corner recirculation zone (CRZ) near the upper corner provoked by the rather sudden enlargement of the cross-sectional area. Of special concern was the characterization of flows of this type in terms of the effects of side-wall angle α, degree of swirl ϕ, inlet expansion ratio D/d, and downstream contraction area ratio A/a on the flowfield in terms of its time-mean and turbulence quantities.

The general goal of this study was to perform experiments and complementary computations with the idea of doing the type of research necessary to improve calculation capability. The goals of the research included:

1) Measurements of mean flow patterns and sizes and shapes of the corner and central recirculation zones.

2) Flowfield mapping of time-mean velocity, normal and shear Reynolds stresses and, hence, turbulent viscosities in each (i,j) orientation.

3) Development of a computer program based on the Imperial College TEACH-T program for two-dimensional axisymmetric, swirling confined jet flows with recirculation regions.

4) Improvement of turbulence models for general swirling recirculating flows, including nonisotropic simulation.

The Present Contribution

Three Ph.D. theses[1-3] (also available as NASA contractor reports) and five M.S. theses[4-8] evolved in connection with this study. In addition, conference papers[9-21] were written and presented on various aspects of the work. Also, one additional NASA contractor report[22] and one subcontractor report[23] were published during the course of this investigation. The NASA final report[24] includes all the conference papers in appendixes. The present paper reviews these activities.

In the experimental portion of the research, a logical sequence of experiments was undertaken to establish the effects on the resulting flowfield of swirler performance and swirl strength, downstream nozzle, expansion ratio, and inlet side-wall angle. Complementary computations were performed

Presented as Paper 85-0184 at the AIAA 23rd Aerospace Sciences Meeting, Reno, NV, Jan. 14-17, 1985; received May 30, 1985; revision submitted Sept. 26, 1985.

*Professor, School of Mechanical and Aerospace Engineering. Associate Fellow AIAA.

corresponding to all the boundary conditions of the experiments so as to provide a thorough evaluation of state-of-the-art predictive capability, with standard and modified turbulence models.

Section II describes facilities and techniques used in the investigation. Section III concentrates on results obtained, with highlights of recent Ph.D. and M.S. theses being included, along with discussion of the coverage of relevant conference papers written during the course of the study. The closure summarizes the study in Sec. IV.

II. Facilities and Techniques

Facilities

Oklahoma State University has the following facilities that were purchased and/or constructed by students during the project:

1) Wind tunnel,
2) One variable-angle vane swirler,
3) Three plexiglass text sections of diameters 30, 22.5, and 15 cm,
4) Expansion blocks of 90 and 45 deg, for each of the three test sections,
5) Weak and strong downstream contraction nozzles for each of the three test sections.

The experiments were conducted in the confined jet test facility, which has an axial-flow fan whose speed can be changed by altering a varidrive mechanism. Numerous fine screens and straws produce flow in the settling chamber of relatively low turbulence intensity. The contraction section leading to the test section has been specially designed to produce a minimum adverse pressure gradient on the boundary layer and thus avoid unsteady problems associated with local separation region. The sudden expansion consists of a 15 cm diam circular jet nozzle, exiting abruptly into a 30 cm diam test section of length 125 cm, which is constructed of plexiglass to facilitate flow visualization. Test sections of 22.5 and 15 cm diam have also been investigated. The side-wall angle α and swirl vane angle ϕ are variable. The side-wall angle is set by inserting a block with side-wall angle α of 90 or 45 deg. Typical operating Reynolds numbers (based on inlet average velocity and inlet diameter) are in the range 50,000 to 150,000, depending upon fan speed and aerodynamic blockage of the swirl vanes. It has been observed that this is approximately in the Reynolds number insensitive range for this facility, in terms of nondimensional flow characteristics further downstream.[1]

Measurement Techniques

Flow visualization techniques included neutrally-buoyant helium-filled soap bubbles, smoke-wire, tufts, and multispark method, with appropriate illumination and photography techniques. For detailed measurements, pitot probe and hot-wire techniques have been used. One of the simplest instruments capable of simultaneously sensing both magnitude and direction of the local velocity vector is the five-hole pitot probe, used extensively in this study.[10,12,15,21] The second measurement technique used extensively was the six-orientation, single-wire hot-wire technique.[11,14,16] The six-orientation technique permits time-mean and turbulence data to be taken in general flowfields. Hot-wire anemometry with multiwire probes have also been used in the study. A crossed hot-wire technique was used in the nonswirling flow.[20] A triple-wire hot-wire technique was developed using a three-wire hot-wire probe with direct computer interface and data reduction.[23]

Prediction Techniques

A primitive pressure-velocity variable finite difference computer code was developed to predict swirling recirculating inert turbulent flows in axisymmetric combustors in general, and for application to the present specific idealized combustion chamber with sudden or gradual upstream expansions and weak or strong downstream contraction nozzles. The development was based on the 1974 Imperial College TEACH-T computer code. The finally developed computer program (written in FORTRAN 4) was code-named STARPIC (mnemonic for swirling, turbulent, axisymmetric, recirculating flows in practical isothermal combustor geometries). The complete report[22] included a program listing and a sample case computation of airflow through a 45 deg expansion ($\alpha = 45$ deg) from an inlet pipe to a larger pipe ($D/d = 2$). This code has been used extensively for a wide variety of combustor configurations and flow conditons, as given in Refs. 1 and 3.

III. Results

Swirler Performance

Throughout the entire research project, the swirler being used was annular with a hub-to-swirler diameter ratio of 0.25 and ten adjustable vanes of pitch-to-chord ratio 0.68. Measurements of time-mean axial, radial, and swirl velocities were made in Refs. 6 and 15 at the swirler exit plane using a five-hole pitot probe technique with computer data reduction. Nondimensionalized velocities from both radial and axiumthal traverses were plotted for a range of swirl vane angles ϕ from 0 to 70 deg. A theoretical study was included of idealized exit-plane velocity profiles relating the swirl numbers S and S' (defined with and without pressure contributions, respectively) to the ratio of maximum swirl and maximum axial velocities for each idealized case.

The nonswirling case shown in Fig. 1a has a nearly flat axial velocity profile, as expected for the plain nozzle opening without the swirler installed. There is no measurable swirl velocity, and the radial velocity is zero except for points very near the edge of the exit, where the flow begins to anticipate the abrupt expansion to twice the exit diameter. The traverse was made midway between two blades and away from any of the hub supporting struts. Here again, the axial profile is quite flat, with just a slight increase toward the hub. However, the velocity has increased by nearly 25% because of the decrease in flow area with swirler hub and vanes in place. In addition, the hub includes a negative radial velocity across the entire annulus, overriding the tendency to anticipate the expansion corner. The swirl velocity is, as expected, negligible.

In the $\phi = 45$ deg case of Fig. 1b, the flat segments are no longer present and both axial and swirl profiles vary from zero at the hub to a maximum at or near the rim of the swirler in an almost linear fashion. The similar shape and magnitude of the profiles indicate that the turning angle is fairly uniform and only slightly less than 45 deg. The radial velocity is again irregular but shows a step at $r/D = 0.1$ similar to that in the axial and swirl profiles, probably because the central recirculation zone downstream is beginning to slow down the flow upstream of it.

Exit velocity profiles obtained for the strongest swirl case considered ($\phi = 70$ deg) are shown in Fig. 1c. Almost all the flow leaves the swirler at the outside edge. The maximum axial and swirl velocities are approximately 3 and 2.5 times the upstream reference values, respectively, and the velocity gradients across the profiles are quite large. The reverse flow in the center of the axial profile is stronger than in the 60-deg case and is now accompanied by negative or inward radial velocity. This suggests the possibility of a vortex ring structure occurring at the exit of the swirler under high-swirl conditions. The swirl velocity profile remains positive but shows a step corresponding to the outer boundary of the recirculation zone.

Measurements at the swirler exit plane show clearly the effects of centrifugal forces, recirculation zones, and blade wakes on the exit-plane velocity profiles. Assumptions of flat axial and swirl profiles with radial velocity equal to zero were found to be progressively less realistic as the swirler blade angle increases. At low swirl strengths ($\phi = 38$ deg), portions of the u and w profiles remain flat while the v component is already significant. At moderate swirl, $\phi = 45$ deg, linearly in-

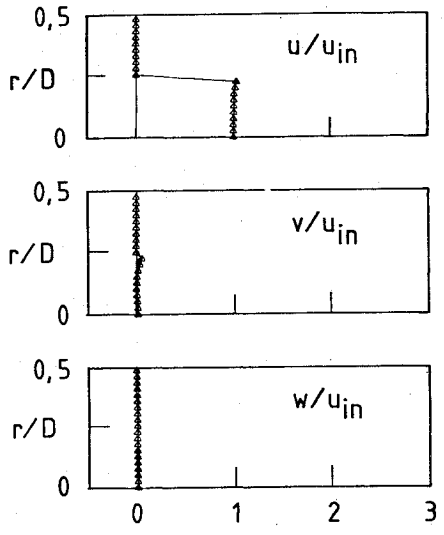

(a) Swirl vane angle $\phi = 0$ deg (no swirler).

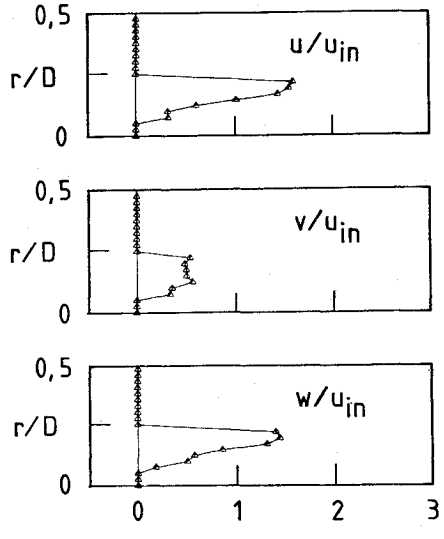

(b) Swirl vane angle $\phi = 45$ deg.

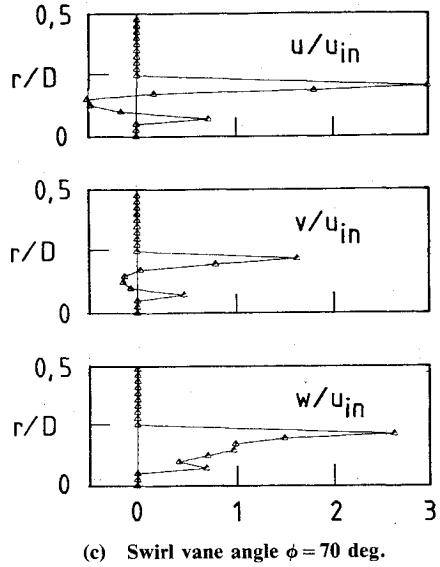

(c) Swirl vane angle $\phi = 70$ deg.

Fig. 1 Normalized swirler exit velocity profiles from radial traverse.

creasing profiles of u and w with radius are appropriate, with v nonzero. At stronger swirl, $\phi = 60$ deg, even more spiked profiles are appropriate, with most of the flow leaving the swirler near its outer edge and with some reverse flow near the hub. At strong swirl, $\phi = 70$ deg, the profiles are extremely spiked, with flow reversal. The central recirculation zone extends upstream of the exit plane, almost to the swirler blades in high-swirl cases. Because of this recirculation, none of the idealizations considered could model strong swirl cases adequately. The flow-turning effectiveness of the flat blades was generally adequate for all vane angles tested. However, the large variations of flow angles and velocities with radius made meaningful comparisons with two-dimensional cascade data impossible. Nonaxisymmetry was found in all swirl cases investigated. It is clear that the investigation of vane swirler performance characteristics served in subsequent parts of the project to aid in computer modeling of gas-turbine combustor flowfields and in the development and evaluation of turbulence models for swirling confined flow.

Gross Flowfield Characterization

Recirculation zones are important to combustor designers, and the size and location of these regions in the present isothermal flows are readily deduced from flow visualization photographs of tufts, smoke, bubbles, and multisparks responding to the experimental flowfield patterns. Resulting dividing streamline sketches, as well as selected photographs of the visualization experiments, are presented and discussed in Refs. 1, 8-10, and 21. In the early part of the study,[1,10] a major outcome was the experimental characterization of corner and central recirculation zones in six basic configurations of an axisymmetric expansion with side-wall angle $\alpha = 90$ and 45 and swirl vane angle $\phi = 0$ (swirler removed), 38, and 45 deg. The size and shape of the recirculation bubbles for each flowfield are illustrated through an artistic impression derived from a collection of flow visualization photographs of tufts, smoke, and neutrally buoyant soap bubbles responding to the flow. Increasing swirl vane angle ϕ from 0 to 38 deg produces a shortened corner region and the appearance of a central bubble typically extending downstream to approximately $x/D = 1.7$, after which a processing vortex core (PVC) exists near the axis reaching to the exit of the test section. A further increase in ϕ to 45 deg enlarges the central zone and vortex core with negligible effect on the corner region in those flowfields where it occurs. The effect of side-wall angle α on the nonswirling flows is negligible. However, a decrease from 90 to 45 deg apparently eliminates the corner recirculation in the swirling flow cases investigated. This decrease in α also causes the inlet flow to impinge more severely on the top wall, where larger axial velocities occur.

Later work[8] continued the flow visualization study for higher swirl strengths, smaller-diameter tubes, and downstream contraction nozzle effects. Nonswirling and swirling inlet flows were investigated in axisymmetric test sections with expansion ratio 1 and 1.5 and the following geometric parameters: side-wall expansion angle $\alpha = 45$ and 90 deg; swirl vane angle $\phi = 0$ (swirler removed), 45, and 70 deg; and downstream blockages of area ratios 2 and 4 located 1 and 2 diameters from the test section inlet. Discussion of significant findings from the flow visualization and pitot probe measurements follow.

Time-Mean Flowfield Characterization

Initial work by Rhode[1,10] utilized the five-hole pitot probe technique to measure time-mean velocities u, v, and w in the large-diameter test section with $D/d = 2$, low swirl strengths $\phi = 0$ (swirler removed), 38, and 45 deg, and no downstream nozzles. Later, Yoon[5,12] extended the study to higher swirl strengths $\phi = 60$ and 70 deg and downstream nozzle effects

with both weak and strong nozzles of area ratios $A/a=2$ and 4 located at $x/D=1$ and 2. Velocities were extensively plotted and artistic impressions of recirculation zones were presented. Findings included the fact that the nonswirling confined jet possesses a corner recirculation zone extending to just beyond $x/D=2$ with no central recirculation zone. The presence of a swirler shortens the corner recirculation zone and generates a central recirculation zone followed by a precessing vortex core. The effect of a gradual inlet expansion is to encourage the flow to remain close the the side wall and shorten the extent of the corner recirculation zone in all cases investigated. A contraction nozzle of area ratio 2 has little effect on weakly swirling and strongly swirling flows, which are dominated by forward flow and centrifugal forces, respectively. For intermediate swirl cases, the weak downstream nozzle encourages foward movement of otherwise slow-moving air and thereby shortens the central recirculation zone. A strong contraction nozzle of area ratio 4 has a more dramatic effect on the flowfields, particularly affecting both intermediate and strong swirling flow cases. Central recirculation zones are shortened considerably, and axial velocities near the facility axis become highly positive. Core regions become narrower with very strong swirl velocity magnitudes and gradients.

Figure 2a-c shows the axial and swirl velocity profiles for $\phi=0$, (swirler removed), 45, and 70 deg, respectively, with side-wall expansion angle $\alpha=90$ deg. The nonswirling flow investigated is obtained with the swirler removed. Figure 2a shows a uniform axial velocity entering the test section. The corner recirculation zone extends to just beyond $x/D=2.0$. Measurements for a corresponding flow were taken with a stagnation tube and pitot tube by Chaturvedi.[25] He found the reattachment point to be at $x/D=2.3$, which is in good agreement with the present study. Moon and Rudinger[26] located the reattachment point with both theoretical and experimental methods in a similar circular test section with an expansion ratio $D/d=1.43$, which is different from the present study (with $D/d=2$). The result yielded a value of $x/D=1.25$ as a reattachment point, which corresponds to an attachment point approximately eight step heights downstream, which is in good agreement with the present study.

The velocity profiles for swirling flows shown in Fig.2b and c reveal that the flow exiting from the swirl vanes is not uniform and has steep velocity gradients in the radial direction, especially at high swirl strengths. Furthermore, a considerable backflow around the hub is observed for $\phi=70$ deg, as shown in Fig. 2c. For all values of swirl vane angle used in this study, the corner recirculation zone does not extend beyond $x/D=0.5$, the closest axial location to the expansion block; instead, the maximum axial velocity is observed close to the top wall at $x/D=0.5$. These effects result from the strong centrifugal forces present in the incoming swirling flow.

The central recirculation zone and processing vortex core (PVC) are now discussed. The precessing vortex core is a region of high swirl, low axial velocity flow along the axis, which has a relatively constant small diameter. In flow visualization studies,[10] it is seen to precess around the axis of the test section. The central recirculation zone is the wide reverse flow region encountered near the inlet. The size of the central recirculation zone increases with the increasing swirl vane angle until a certain value of swirl vane angle is reached (around 40 deg). Then its length begins to decrease under stronger swirl conditions, but its width continues to increase. The core vortex was present at all values of swirl vane angle used in this investigation. In contrast to the central recirculation zone, the vortex core widens continuously as the swirl strength increases.

The swirl velocity peaks sharply around the edge of the expansion block before becoming more uniform further downstream as shown in Fig. 2b and c. A considerably nonuniform swirl velocity profile is observed at $x/D=0.5$. Thereafter, relatively steady and uniform velocity profiles are seen, except for the region around the axis. The radial location

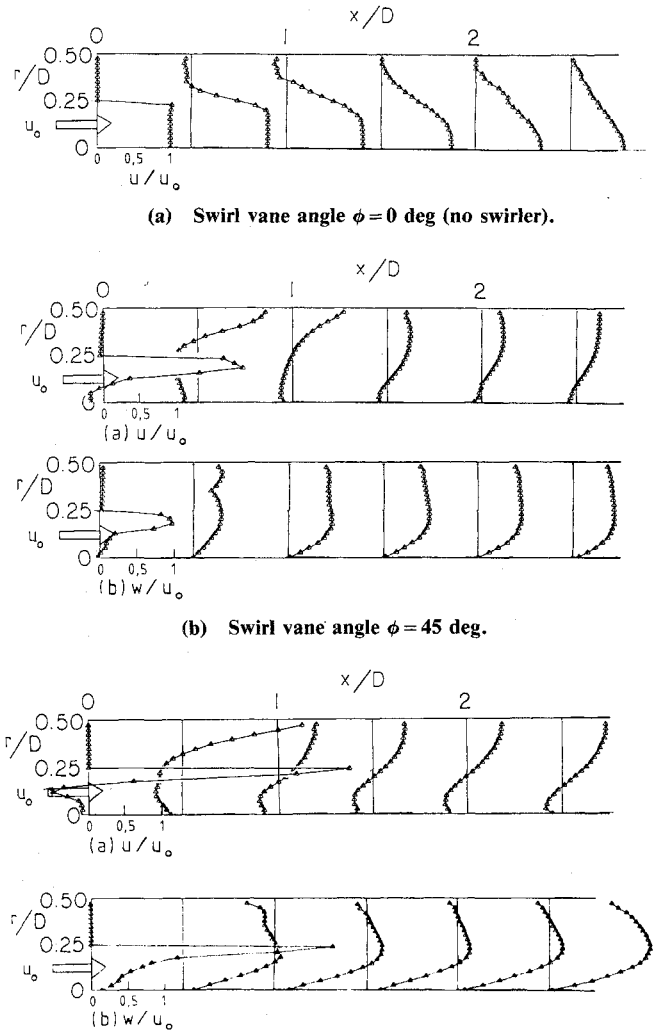

Fig. 2 Velocity profiles for side-wall expansion angle $\alpha=90$ deg without contraction nozzle for flowfield with $D/d=2$.

of maximum swirl velocity nears the outer edge of the swirler as the swirl vane angle increases. This trend is caused by the increase of centrifugal effects. The swirl velocity along the axis is found to be zero as expected because of symmetry.

The effect of a strong contraction nozzle was investigated for a range of swirl strengths $\phi=0$, 45, and 70 deg with side-wall expansion angle $\alpha=90$ deg. The contraction nozzle, of area ratio 4 with 45 deg sloping upstream face, was located at $x/D=1$ and 2. Figure 3a-c shows these velocity profiles with $x/D=2$ only, while results with $x/D=1$ appear in Ref. 5. Figure 3a shows that the flowfield with a strong contraction nozzle changes very little as compared to the corresponding flowfield with, or without, a weak contraction nozzle. Figure 3b shows the axial and swirl velocity profiles for a swirl vane angle $\phi=45$ deg. The presence of a strong contraction nozzle generates a high positive axial velocity near the axis at all axial locations. However, it decelerates the axial velocity close to the top wall. The central recirculation zone is much smaller than previous corresponding cases, and it is located in an annular region. The swirl velocity profiles show narrower core regions with stronger swirl velocity magnitudes and gradients than previously. For swirl vane angle $\phi=70$ deg, the axial and swirl velocity profiles are given in Fig. 3c, with the strong contraction blockage located at $x/D=2$. The axial velocity near the axis is highly positive and the central recirculation region is very small, extending in an annular region to less than

$x/D=1$, much less than its corresponding case with the weak contraction block and considerably less than the no-blockage case. At the axial station $x/D=1$, forward flow occurs across the whole test section. This situation is in sharp contrast to that of a weak contraction nozzle, in which case the contraction block affects the flowfield very little under strong swirling conditions, with centrifugal effects dominating. Swirl velocity profiles given in Fig. 3c show the even narrower core than at $\phi=45$ deg with very strong swirl velocity magnitudes and gradients. Summarizing, whereas the effect of a weak contraction nozzle of area ratio 2 is confined to intermediate swirl cases, a strong contraction nozzle of area ratio 4 affects both intermediate and strongly swirling flow cases.

More recently, Scharrer[8,21] used the same measurement technique with smaller-diameter test section tubes with $D/d=1.5$ and 1, again with downstream nozzles and a full range of swirl strengths. It was found that the corner recirculation zone is prominent in nonswirling expanding flows but decreases when swirl is introduced. The presence of swirl results in the formation of a central recirculation zone. Initially, increases in inlet swirl strength result in an increase in length of this zone. However, increasing to very high swirl strengths results in shortening and widening of this zone. Placing a downstream nozzle in the flowfield creates an adverse pressure gradient near the wall and a favorable pressure gradient near the centerline. This results in increased axial and swirl velocities near the centerline and decreased velocities near the wall. It also decreases the central recirculation zone length. The degree of the effect increases as the degree of blockage increases. Reduction of the expansion ratio results in a reduction of the central recirculation zone length. The corner recirculation zone length (measured in step heights) does not change appreciably with expansion ratio for ratios greater than 1. Gradual expansion has a minimal effect on the flow.

The velocity profiles in Fig. 4a-c show how the flowfield of Fig. 2 changes when the expansion ratio is reduced to 1. The axial velocity in Fig. 4a is merely plug flow. Centrifugal effects dominate the axial and swirl profiles of Fig. 4b and c. The highest velocities are located farthest from the centerline. The profiles change very little as they move downstream. In addition, there is no flow recirculation for the moderate swirl case and only a small central toroidal recirculation zone (CTRZ) extending to $x/D=0.5$ for the strong swirl case.

Concerning the corner recirculation zone (CRZ), after comparing the present data for $D/d=1.5$ with the data of Yoon[5] and Moon and Rudinger,[26] and data tabulated by Sinder and Harsha,[27] it can be seen that the reattachment point for a suddenly expanding nonswirl flow is found to be between 6 to 9 step heights downstream of the inlet regardless of the expansion ratio. Table 1 amalgamates the data, to show the consistency of reattachment point location for $D/d>1$.

Table 2 shows the variation of CTRZ length with expansion ratio, using the present data and that of Ref. 5. The data show no clear trend for moderate swirl: The CTRZ length decreases from 1.6 to 1.5 to 0 diameters as the expansion ratio decreases from 2 to 1.5 to 1. However, there is a steady decrease in

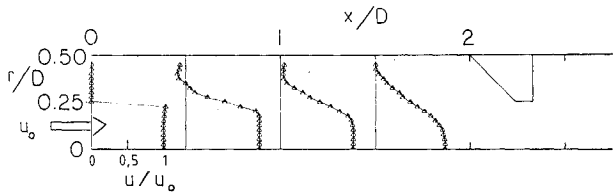

(a) Swirl vane angle $\phi=0$ deg (no swirler).

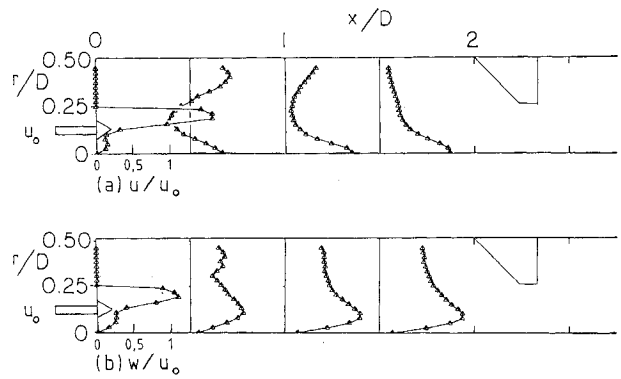

(b) Swirl vane angle $\phi=45$ deg.

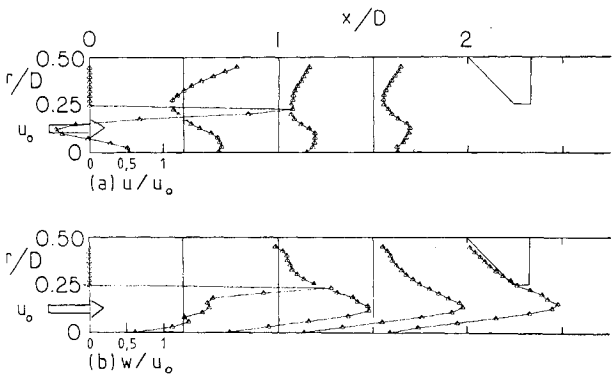

(c) Swirl vane angle $\phi=70$ deg.

Fig. 3 Velocity profiles with strong contraction nozzle of area ratio 4 located at $x/D=2$ for flowfield with $D/d=2$.

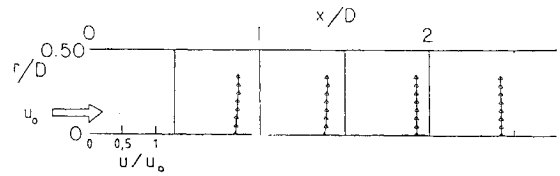

(a) Swirl vane angle $\phi=0$ deg (no swirler).

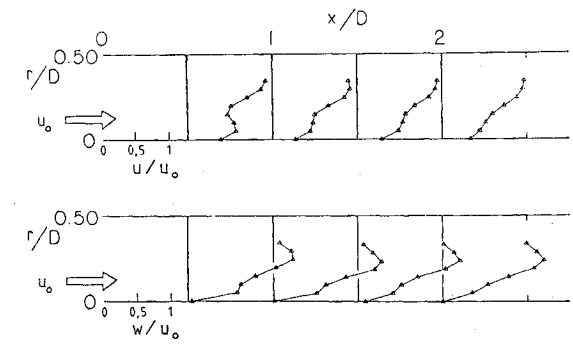

(b) Swirl vane angle $\phi=45$ deg.

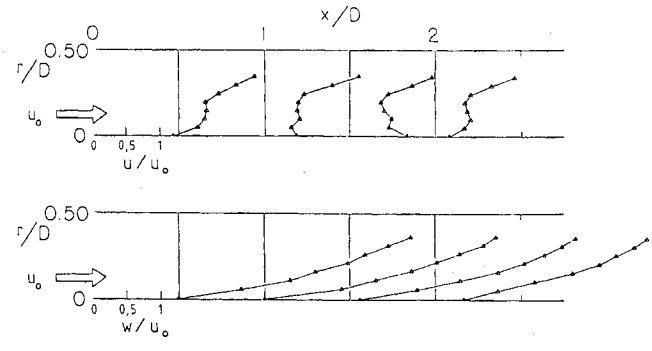

(c) Swirl vane angle $\phi=70$ deg.

Fig. 4 Velocity profiles for open-ended flow with $D/d=1$.

Table 1 Corner recirculation zone lengths for nonswirling flow

Expansion ratio, D/d	CRZ length in step heights
1.43	8
1.5	7.5
1.73	8
2	8
3	6.25

Table 2 Central recirculation zone lengths (x/D) for swirling flow

D/d	$\phi=45$	$\phi=70$
1.0	0	0.5
1.5	1.5	0.75
2.0	1.6	1.2

CTRZ length for strong swirl, which goes from 1.2 to 0.75 to 0.5 diameters as the expansion ratio goes from 2 to 1.5 to 1. In general, the length of the CTRZ decreases as the expansion ratio decreases, and this effect becomes more pronounced as the swirl strength increases.

Reducing the expansion ratio to 1 results in the flowfield alterations shown in Fig. 5a-c. The nonswirling flow of Fig. 5a exhibits the familiar change: induced swirl near the blockage and centerline acceleration. For the moderate swirl of Fig. 5b, the velocity profiles show large increases in centerline axial and swirl velocities to be diminished near-wall velocities. The strong swirl flow of Fig. 5c shows that the centerline axial velocities at $x/D=0.5$ and 1 are negative; the off-centerline axial and swirl velocities are very large; and the axial and swirl velocities diminish near the wall.

Correlating the present data with that of Ref. 5 for $D/d=2$, it is clear that the effect of a blockage is to accelerate the axial and swirl velocities near the centerline, diminish those velocities near the wall, and decrease the length of the CTRZ. The effect is greater when the degree of blockage is greater. For strong swirl flows, a blockage increases the length of CTRZ when the expansion ratio is 1. Otherwise (that is, $D/d>1$), a blockage shortens the CTRZ.

Turbulence Measurements

Major attention was given to the development and application of the six-orientation, one-wire hot-wire technique in the present confined jet facility. Applied in this study to nonreacting flowfields, deductions of time-mean velocities, turbulence intensities, and shear stresses were possible. The experiments were performed to provide the information necessary for turbulence modeling development in the confined jet facility. Initially, the mathematics and computer reduction code for the technique were developed for the nonswirling flow;[4] later, the validity of the technique was established for the swirling flowfield with inlet swirl vane angle of 38 deg.[11] Excellent cost-effective results were presented, with comparisons with independent data illustrating the reliability of the technique. Finally, a sensitivity analysis of the data reduction technique was undertaken, which formed the major ingredient of an uncertainty analysis.[11]

Jackson[2] further applied the technique for a full range of swirl strengths in the test section with expansion ratios $D/d=1$ and 2, which may be equipped with a strong contraction nozzle of area ratio 4 at $x/D=2$. The effect of swirl on time-mean velocities and complete Reynolds stress tensor was investigated, and extensive results were given for swirl vane angles of 0 (swirler removed), 38, 45, 60, and 70 deg. Dissipation rates were also measured. Major results were reported for

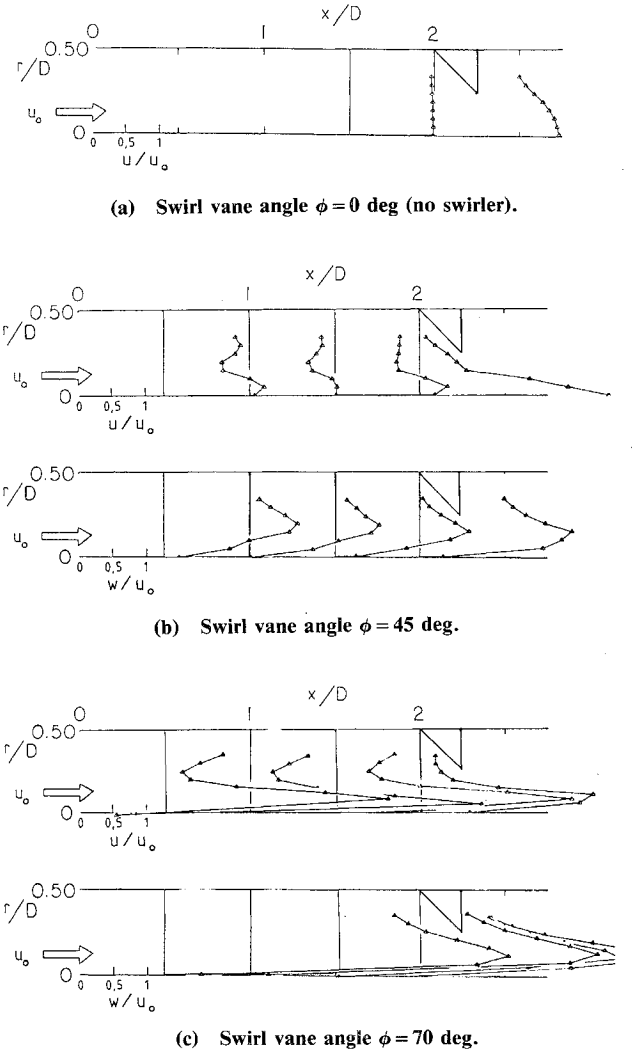

(a) Swirl vane angle $\phi=0$ deg (no swirler).

(b) Swirl vane angle $\phi=45$ deg.

(c) Swirl vane angle $\phi=70$ deg.

Fig. 5 Velocity profiles for flow with $D/d=1$ and strong contraction nozzle of area ratio 4 located at $x/D=2$.

the expansion flowfield in Ref. 14. The effect of swirl on the time-mean velocity field was found to shorten the length of the corner recirculation zone (CRZ) and to generate the existence of a central toroidal recirculation zone (CTRZ), which is followed by a precessing vortex core (PVC) region. As the degree of swirl increases, the length of the central recirculation bubble decreases, whereas its width, and also the width of the PVC, increases. At the jet inlet to the test section, directional turbulence intensities are found to increase significantly with swirl. Throughout the flowfield, the most dramatic effect of swirl is to increase values of the three turbulent shear stress terms. The extensive results are plotted and tabulated in Ref. 2. In general, time-mean velocity measurements and flowfield patterns confirm those found earlier using the five-hole pitot probe technique.

Figure 6 shows time-mean and turbulence data for the strongest swirl case considered in the large tube with $D/d=2$ and inlet swirl vanes at an angle of $\phi=70$ deg. Corresponding data for other swirl strengths, downstream nozzle effects, and the smaller test section with $D/d=1$ are given in Refs. 2 and 14. Almost all of the flow leaves the swirler near the outer edge, producing steep velocity gradients in this vicinity. High velocity gradients can also be seen near the wall, expecially at $x/D=0.5$. The strong centrifugal forces present in the incoming flow produce rapid outflow to the confining boundary. Both central and corner recirculation zones can be seen clearly from the time-mean plots. However, it appears that the CTRZ is shorter for this strong degree of swirl as compared to the

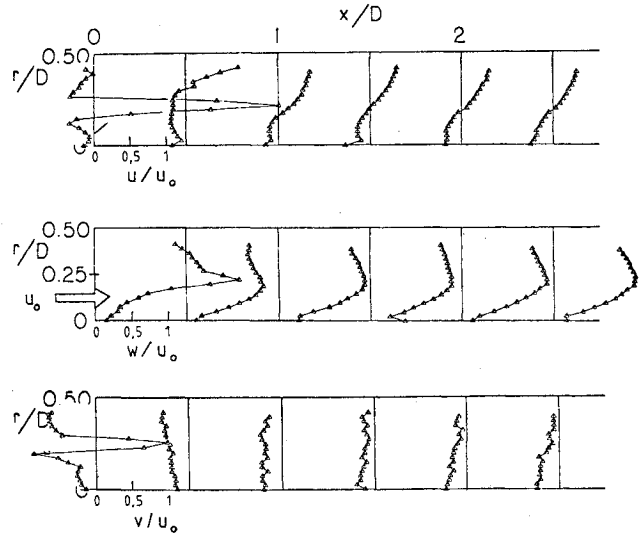

(a) Time-mean velocities.

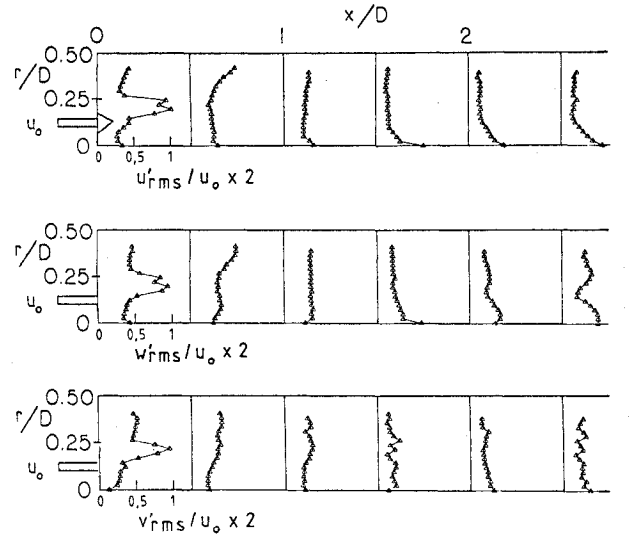

(b) Normal stresses.

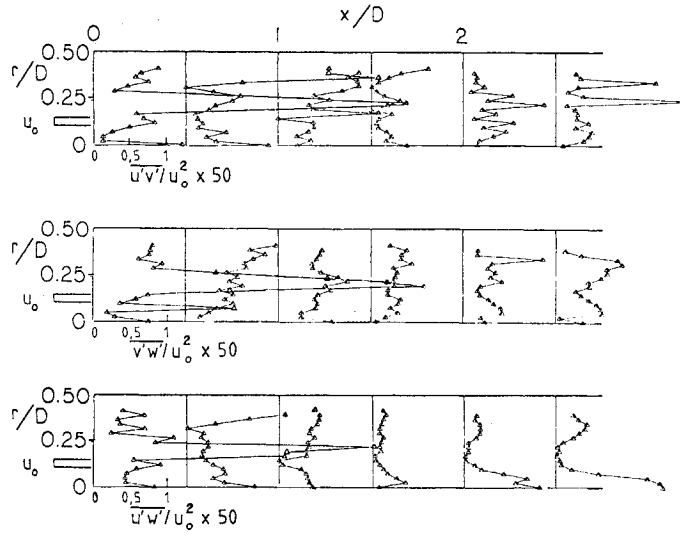

(c) Shear stresses.

Fig. 6 Time-mean and turbulent data for $D/d=2$ flowfield with swirl vane angle $\phi=70$ deg.

moderate swirl case. In contrast, the PVC gets wider as the swirl strength increases, as also found in five-hole pitot probe data.[12]

The normal turbulent stresses have increased in magnitude, consistent with the increase in swirl strength, and still a good degree of isotropy is observed throughout the entire flowfield. The highest turbulence levels again occur in regions of recirculation and on the shear layers. It can also be seen that high turbulence levels are found in the PVC.

The most dramatic effect of the increase of swirl is the large increase in all three shear stress values. Very high values of shear stress occur in the shear layers and near the walls. The PVC also contains high values of shear stresses and turbulence levels. Overall, the values of shear stresses are higher at the stronger swirl strengths.

Introduction of a strong contraction nozzle at $x/D=2$ with an area reduction ratio of 4 causes a significant effect on the time-mean swirling flowfield. Central recirculation zones are shortened and axial velocities along the whole jet axis become positive. The core regions become narrow with strong swirl velocities and gradients. Turbulence levels and shear stresses also increase along the jet centerline near the exit of the contraction nozzle.

The accuracy and directional sensitivity of the technique were also assessed, with respect to mean flow velocity orientation to the probe, (see Ref. 16). Results demonstrate relative insensitivity, indicating that the method is a useful cost-effective tool for turbulent flows of unknown dominant flow direction. The technique adequately measures the properties of a flowfield independent of the dominant flow direction except when the flow is predominantly in the direction of the probe holder, with the six-orientations of the probe then creating insignificant changes in hot-wire response.

A crossed hot-wire technique had been used for the nonswirling free and confined jet ($D/d=2$) situations.[7,20] Axial and radial time-mean velocities, directional turbulence intensities, and main Reynolds stress were measured. Associated turbulent viscosity values were deduced throughout. Investigations were made with and without a downstream contraction nozzle of area ratio 4 located at $x/D=2$. Measurements indicated that the crossed hot-wire used cannot handle axial flow reversal (without prior knowledge and probe reorientation) and that the experimental technique is inadequate for the measurement of time-mean radial velocity. Other quantities show a high level of comparability. In common with previous researchers, time-mean and turbulence characteristics with the contraction nozzle at $x/D=2$ show little change from that of the corresponding flowfield without a contraction nozzle for the nonswirling flow case.

Turbulence Modeling

Abujelala[3] continued the earlier prediction work of Rhode[1] and, additionally, stressed turbulence modeling possibilities. In Ref. 17 shortcomings and recommended corrections to the standard two-equation k-ϵ turbulence model suggested by previous investigators were presented. They were assessed regarding their applicability to turbulent swirling recirculating flow. Recent experimental data on swirling confined flows, obtained with a five-hole pitot probe and a six-orientation hot-wire probe, were used to obtain optimum values of the turbulence parameters C_μ, C_2, and σ_ϵ for swirling flows, using an effective optimization code called the Hill Algorithm.[28] General predictions of moderately and strongly swirling flows with these optimized values are more accurate than predictions with the standard or previous simple extensions of the k-ϵ turbulence model.

The detailed data base evolved in the course of recent studies were analyzed numerically as a contribution to the turbulence modeling effort.[18] Swirl strength and a strong contraction nozzle were found to have strong effects on the turbulence parameters. Generally, the most dramatic effect of the increase of swirl is the considerable increase in all the

parameters considered—that is, in particular, increase of turbulent viscosity and kinetic energy. The presence of a strong contraction nozzle tends to increase parameter values in regions of acceleration where large radial velocity gradients occur and to reduce them in the deceleration region near the outer boundary. Based on similarity of viscosity and length scale profiles, a C_μ formulation was deduced in which

$$C_\mu = Au_0/k^{1/2} \tag{1}$$

where A is a constant independent of spatial position in the flow. Using an optimization procedure similar to that described in Ref. 17, optimal values of A, C_2, and σ_ϵ have been deduced for the present situaiton. It was found that

$$A = 0.0083,\ C_2 = 1.804,\ \sigma_\epsilon = 1.455 \tag{2}$$

The flowfields for inlet swirl vane angles of $\phi = 45$ and 70 deg have been predicted using the C_μ variation as given by Eq. (1), with the optimized values of Eq. (2) used in this and other equations occurring in the simulation. This formulation was shown to improve the predictive capability of the standard k-ϵ turbulence model in swirling recirculating flows.[19]

Computer Predictions

Application of the STARPIC computer code[22] was made to the simulation of isothermal airflow in the axisymmetric test facility with diameter expansion ratio D/d of 2, with two wall expansion angles α of 90 and 45 deg and three swirl vane angles ϕ of 0, 45, and 70 deg. All results were obtained via a nonuniform grid system so as to enhance solution accuracy. The inlet profiles of axial velocity u and swirl velocity w are idealized as "flat" (that is, constant-valued). Predicted u and w velocity profiles for the six flowfield configurations are given in Refs. 1 and 9, together with deduced parametric effects on recirculation zone lengths. The general trends are similar to the experimental findings.

Abujelala[3] continued the theoretical study and assessed the validity of flowfield predictions resulting from the choice of inlet velocity profiles. Results[13] demonstrated that realistic predictions are forthcoming only from the inclusion of realistic axial, radial, and swirl velocity profiles as inlet, conditions. Predictions with flat inlet profiles, solid body rotation, or zero radial velocity are inappropriate. Predictions were given for a full range of swirl strengths using measured inlet axial, radial, and swirl velocity profiles in each case, and predicted velocity profiles, streamline plots, and axial velocity representations illustrated the large-scale effects of inlet swirl on flowfields. Results generally confirm the well-known ideas about swirl effects on axisymmetric turbulent confined jet flows.[29]

Predictions were included for the effect of weak and strong downstream contraction nozzles on the flow. In the swirl flow cases, a weak nozzle leads to the discouragement of central recirculation zones with stronger vortex cores downstream possessing negative axial velocities. A strong nozzle has more pronounced effects on swirl flow cases, with discouragement of central recirculation zones, and forward flow in highly swirled vortex core regions further downstream. Under nonswirling conditions, the blockage effect is minimal—the central forward flow is accelerated and the large corner recirculation remains.

Later production runs given in Ref. 19 included predictions of swirl, confinement, and nozzle effects on confined turbulent flow, which were exhibited and compared with five-hole pitot-probe time-mean velocity measurements of Refs. 12 and 21. Comparisons were also possible with the time-mean velocities found in the hot-wire study of Refs. 2 and 14. Two sets of computations were given, one using the standard k-ϵ turbulence model and the other using a C_μ-formulation model deduced from six-orientation, single-wire hot-wire measurements, as discussed in the preceding subsection. Results confirmed that the accuracy of the latter model is superior. To highlight the effects of confinement and exit nozzle area on this flow, three expansion ratios and two contraction ratios were used. Predictions were given for a full range of swirl strengths using the measured inlet conditions of Ref. 15 for axial, radial, and swirl velocity profiles. The predicted velocity profiles illustrate the large-scale effects of inlet swirl on the flowfields. It appears that a strong contraction nozzle has a pronounced effect on swirl flow cases, with discouragement of central recirculation zones, and forward flow in highly swirled vortex core regions. The expansion ratio value has large-scale effects on the size and location of the recirculation zones.

The predicted velocity profiles for inlet swirl vane angles of 0, 45 and 70 deg using the C_μ formulation of Eq. (1) are given and compared with five-hole pitot probe experimental data[12] in Fig. 7. Inspection of this figure reveals that very good agreement between the predicted results and the experimental data has been achieved. Note that the measured inlet profiles are plotted at the $x/D = 0$ location; in fact, these are actually the values measured immediately downstream of the swirler, at the location $x/D = -0.11$. It is convenient to retain these values on the profile plots in the prediction study, although clearly results at the $x/D = 0$ location are then not directly

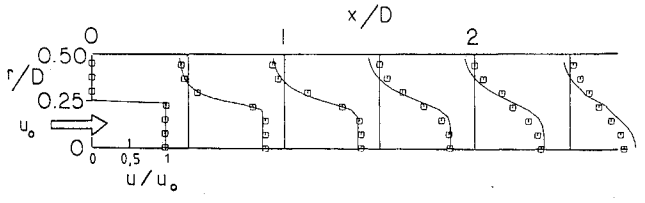

(a) Swirl vane angle $\phi = 0$ deg (no swirler).

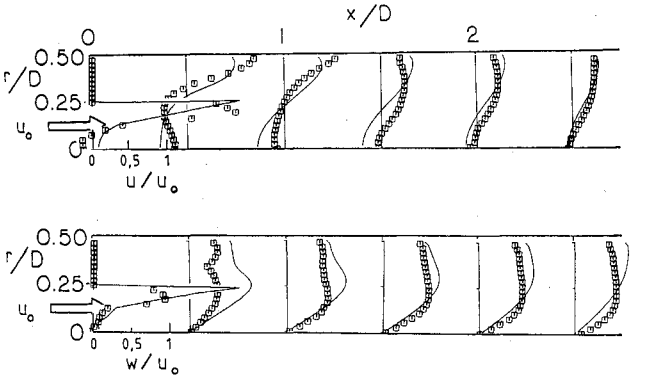

(b) Swirl vane angle $\phi = 45$ deg.

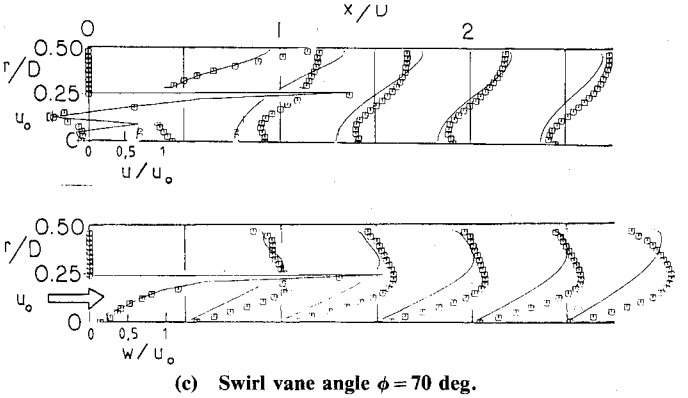

(c) Swirl vane angle $\phi = 70$ deg.

Fig. 7 Measured and predicted velocity profiles using empirical relation of Eq. (1) for C_μ for flowfield with $D/d = 2$ (□ experimental data[2]).

comparable with the inlet station data of Ref. 12, which are taken precisely at $x/D=0$. The discrepancies in the centerline velocity values at the peak of the central recirculation core are expected due to the assumption of axisymmetry at that location in the predictions.

For comparison purposes, predictions using the standard k-ϵ model are also given for the corresponding case in Ref. 18. These yield inaccurate predictions of the size and strength of the recirculation zone. However, predicted results using the C_μ formulation exhibit very good agreement with experimental data, as seen in Fig. 7. Thus, it is clear that the proposed C_μ formulation has provided superior results over the standard k-ϵ model.

Predictions were also given in Ref. 19 for circular cross-sectioned duct flow without inlet expansion. The predicted time-mean results show good agreement with the experimental data of Refs. 2, 8, and 21. Three swirl strengths were considered from zero to strong swirl. No central recirculation zone was found for nonswirling and moderately swirling flows. However, the strongly swirling flow ($\phi=70$ deg) showed a very small central recirculation zone close to the domain inlet. These observations are in accord with expectations and with information about the vortex breakdown phenomenon.[30]

IV. Conclusion

The main objectives of the research program were to determine the effects of swirl and combustor geometry on isothermal flowfield patterns, time-mean velocities, and turbulence quantities and to establish an improved simulation in the form of a computer prediction code equipped with a suitable turbulence model. The study included the investigation of a complete range of swirl strengths, swirler performance, downstream contraction nozzle sizes and locations, expansion ratios, and inlet side-wall angles. Their individual and combined effects on the test section flowfield were observed, measured, characterized, and predicted. The present review paper highlights the findings. Further details appear in the Ph.D. and M.S. theses that have evolved and in the conference research papers that have been written.

Acknowledgments

The author is indebted to NASA Lewis Research Center and Air Force Wright Aeronautical Laboratories for support under Grant No. NAG 3-74, technical monitor, Dr. J.D. Holdeman. The results upon which the present review paper has been based were obtained by various graduate students, under the author's advice (see Refs. 1-8), to whom gratitude is expressed.

References

[1]Rhode, D.L., "Predictions and Measurements of Isothermal Flowfields in Axisymmetric Combustor Geometries," Ph.D. Thesis, Dept. of Mechanical and Aerospace Engineering, Oklahoma State University, Stillwater, OK, Dec. 1981; also Rhode, D.L. and Lilley, D.G., "Predictions and Measurements of Isothermal Flowfields in Axisymmetric Combustor Geometries," NASA CR-174916, May 1985.

[2]Jackson, T.W., "Turbulence Characteristics of Swirling Flowfields," Ph.D. Thesis, Oklahoma State University, Stillwater OK, Dec. 1983; also Jackson, T.W. and Lilley, D.G., "Turbulence Characteristics of Swirling Flowfields," NASA CR-174918, May 1985.

[3]Abujelala, M.T., "Confined Turbulent Swirling Recirculating Flow Predictions," Ph.D. Thesis, Oklahoma State University, Stillwater, OK, June 1984; also Abujelala, M.T. and Lilley D.G., "Confined Turbulent Swirling Recirculating Flow Predictions," NASA CR-174917, May 1985.

[4]Janjua, S.I., "Turbulence Measurements in a Complex Flowfield Using a Six-Orientation Hot-Wire Probe Technique," M.S. Thesis, Oklahoma State University, Stillwater, OK, Dec. 1981.

[5]Yoon, H.K., "Five-Hole Pitot Probe Probe Time-Mean Velocity Measurements in Confined Swirling Flows," M.S. Thesis, Oklahoma State University, Stillwater, OK, July 1982.

[6]Sander, G.F., "Axial Vane-Type Swirler Performance Characteristics," M.S. Thesis, Oklahoma State University, Stillwater, OK, May 1983.

[7]McKillop, B.E., "Turbulence Measurements in a Complex Flowfield Using a Crossed Hot-Wire." M.S. Thesis, Oklahoma State University, Stillwater, OK, July 1983.

[8]Scharrer, G.L., "Swirl, Expansion Ratio and Blockage Effects on Confined Turbulent Flow," M.S. Thesis, Oklahoma State University, Stillwater, OK, May 1984.

[9]Rhode, D.L., Lilley, D.G., and McLaughlin, D.K., "On the Prediction of Swirling Flowfields Found in Axisymmetric Combustor Geometries," *Proceedings of the ASME Symposium on Fluid Mechanics of Combustion Systems*, Boulder, CO, June 22-24, 1981, pp. 257-266; also *ASME Journal of Fluids Engineering*, Vol. 104, Sept. 1982, pp. 378-384.

[10]Rhode, D.L., Lilley, D.G., and McLaughlin, D.K., "Mean Flowfields in Axisymmetric Combustor Geometries with Swirl," AIAA Paper 82-0177, 1982; also *AIAA Journal*, Vol. 21, April 1983, pp. 593-600.

[11]Janjua, S.I., McLaughlin, D.K., Jackson, T.W., and Lilley, D.G., "Turbulence Measurements in a Confined Jet Using a Six-Orientation Hot-Wire Probe Technique," AIAA Paper 82-1262, 1982; also *AIAA Journal*, Vol. 21, Dec. 1983, pp. 1609-1610.

[12]Yoon, H.K. and Lilley, D.G., "Five-Hole Pitot Time-Mean Velocity Measurements in Confined Swirling Flows," AIAA Paper 83-0315, 1983; also *AIAA Journal*, Vol. 22, April 1984, pp. 514-515.

[13]Abujelala, M.T. and Lilley, D.G., "Confined Swirling Flow Predictions," AIAA Paper 83-0316, 1983.

[14]Jackson, T.W. and Lilley, D.G., "Single-Wire Swirl Flow Turbulence Measurements," AIAA Paper 83-1202, 1983.

[15]Sander, G.F. and Lilley, D.G., "The Performance of an Annular Vane Swirler," AIAA Paper 83-1326, 1983.

[16]Jackson, T.W. and Lilley, D.G., "Accuracy and Directional Sensitivity of the Single-Wire Technique," AIAA Paper 84-0367, 1984.

[17]Abujelala, M.T. and Lilley, D.G., "Limitations and Empirical Extensions of the k-ϵ Model as Applied to Turbulent Confined Swirling Flows," AIAA Paper 84-0441, 1984; also *Chemical Engineering Communications*, Vol. 31, 1981, pp. 223-236.

[18]Abujelala, M.T., Jackson, T.W., and Lilley, D.G., "Swirl Flow Turbulence Modeling," AIAA Paper 84-1376, 1984.

[19]Abujelala, M.T. and Lilley, D.G., "Swirl, Confinement and Nozzle Effects on Confined Turbulent Flow," AIAA Paper 84-1377, 1984.

[20]McKillop, B.E. and Lilley, D.G., "Turbulence Measurements in a Complex Flowfield Using a Crossed Hot-Wire," AIAA Paper 84-1604, 1984.

[21]Scharrer, G.L. and Lilley, D.G., "Five-Hole Pitot Probe Measurements of Swirl, Confinement and Nozzle Effects on Confined Turbulent Flow," AIAA Paper 84-1605.

[22]Lilley, D.G. and Rhode D.L., "A Computer Code for Swirling Turbulent Axisymmetric Recirculation Flows in Practical Isothermal Combustor Geometries," NASA CR-3442, Feb. 1982.

[23]Janjua, S.I. and McLaughlin, D.L., "Turbulence Measurements in a Swirling Confined Jet Flowfield Using a Triple Hot-Wire Probe," Report DT-8178-02, Dynamics Technology, Inc., Torrance, CA, Nov. 1982.

[24]Lilley, D.G., "Investigation of Flowfields Found in Typical Combustor Geometries," NASA CR-3869, Feb. 1985.

[25]Chaturvedi, M.C., "Flow Characteristics of Axisymmetric Expansions," *ASCE Proceedings, Journal Hydraulics Division*, Vol. 89, No. HY3, 1963, pp. 61-92.

[26]Moon, L.F. and Rudinger, G., "Velocity Distribution in an Abruptly Expanding Circular Duct," *ASME Journal of Fluids Engineering*, March 1977, pp. 226-230.

[27]Sinder, M.M. and Harsha, P.T., "Assessment of Turbulence Models for Scramjet Flowfields," NASA CR 3643, 1982.

[28]Kuester, J.L. and Mize, J.H., *Optimization Techniques with FORTRAN*, McGraw-Hill Book Co., New York, 1973.

[29]Gupta, A.K., Lilley, D.G., and Syred, N., *Swirl Flows*, Abacus Press, Tunbridge Wells, England, 1984.

[30]Hall, M.G., "Vortex Breakdown," *Annual Review of Fluid Mechanics*, Vol. 4, 1972, pp. 195-218.